PORTLAND CEMENT ASSOCIATION
RESEARCH AND DEVELOPMENT LABORATORIES

Development Department • Bulletin D143

FATIGUE TESTS OF PRESTRESSED CONCRETE PAVEMENTS

By A. P. Christensen and
B. E. Colley

Authorized Reprint from
Highway Research RECORD
Number 239, pp. 175-196 (1968)
Washington, D.C. 20418

FATIGUE TESTS OF PRESTRESSED CONCRETE PAVEMENTS

By A. P. Christensen and
B. E. Colley

PORTLAND CEMENT ASSOCIATION
RESEARCH AND DEVELOPMENT LABORATORIES
Old Orchard Road
Skokie, Illinois 60076

Fatigue Tests of Prestressed Concrete Pavements

A. P. CHRISTENSEN and B. E. COLLEY, Paving Development Section, Portland Cement Association, Skokie, Illinois

The fatigue characteristics of prestressed concrete pavements were studied by repetitive moving load tests on 16 reduced scale prestressed concrete slabs. Each slab was 16 ft long, 12 ft wide, and 1 in. thick. Variables were magnitude of load, amount of longitudinal and transverse prestress, and subgrade strength.

Relationships were established between load magnitude, prestressed pavement properties, and the number of load coverages causing failure. Data from tests on slabs with varying magnitudes of prestress indicate that a minimum prestress of approximately 30 psi in both longitudinal and transverse directions is required to avoid top surface cracking when relatively few moving loads greater than those causing bottom surface cracking are applied repeatedly at interior locations. Data from tests on slabs cast on foundations of different strengths indicated that an increase in the foundation strength resulted in an increase in the number of load coverages causing failure.

KEYWORDS: Deflection; design; fatigue (materials); models; moving loads; prestressed concrete pavements; stresses; subgrade; theories.

•THE LOAD response of prestressed concrete pavements is being studied at the Research and Development Laboratories of the Portland Cement Association. The first published result of this study was a theoretical procedure (1) for determining the magnitude and distribution of stresses and deflections in prestressed concrete pavements for loads beyond cracking of the bottom surface. This procedure is specifically applicable to a centrally loaded infinite slab supported by a "dense liquid" foundation and prestressed equally in longitudinal and transverse directions.

To test the validity of the assumptions made in the theoretical procedure, load tests (2) were conducted on three reduced scale prestressed concrete slabs supported on a coil spring subgrade. Measurements of strain and deflection were made at a number of locations and load increments. Comparisons between test data and theory indicated fair agreement for values of deflection; however, measured strains were significantly smaller than those predicted by theory. The theoretical assumption that the moment-curvature relationship can be represented by two straight lines, an elastic portion with a constant slope followed by a plastic portion in which curvature increases under constant moment, was shown to be conservative for the static type of loading used.

Strain and deflection data were also reported (3) from static load tests conducted on three concrete slabs post-tensioned with steel strands. Each slab was 30 ft long, 12 ft wide, and 5 in. thick. Results again indicated that a prestressed concrete pavement can adequately support an edge or interior load of greater magnitude than that causing bottom surface cracking. Crack patterns were similar to those predicted by the theoretical procedure. Bottom surface cracks extended radially from the center of the load; top surface cracks were approximately circular for interior loads and semicircular for edge loads. However, applications of repeated moving loads cause the development of a random pattern of bottom surface cracks. To obtain information on the fatigue characteristics of prestressed concrete pavements with numerous working bottom surface cracks, a program of repetitive moving load tests was initiated on reduced scale prestressed concrete slabs.

Paper sponsored by Committee on Rigid Pavement Design and presented at the 47th Annual Meeting.

SCOPE AND OBJECTIVES

The test program was designed to study the behavior of 16 prestressed concrete slabs subjected to repetitive moving loads. Variables were magnitude of load, amount of longitudinal and transverse prestress, and subgrade strength. Because it was necessary to test a number of slabs to obtain sufficient data for a fatigue diagram, a reduced scale size was selected for the test slabs and the loading apparatus. The slabs were pretensioned and cast in place on either a clay subgrade, granular subbase, or cement-treated subbase.

The specific objectives of the program were (a) to determine a relationship between the load magnitude and the number of coverages causing pavement failure, (b) to determine the influence of prestress magnitude and foundation strength on fatigue properties of prestressed pavements, and (c) to observe the characteristics of a prestressed pavement failure and determine the factors that cause its development.

TEST FACILITIES AND MATERIALS

Data are reported from load tests on 16 concrete slabs 16 ft long, 12 ft wide, and 1 in. thick. Prestressing was accomplished with pretensioned high-strength steel wire. The slabs were cast in place and tested with a moving load apparatus designed for this program.

Test Area, Subgrade, and Subbase Materials

The prestressed slabs were cast and tested in the area shown in Figure 1. This area is enclosed in a 24-ft wide concrete building equipped with thermostatically controlled heaters to provide uniform temperature during the heating season. The test area was excavated 4 ft below grade to the bottom of the wall footings, and a 5-in. reinforced concrete floor was cast to form an enclosure for a subgrade material. A waterproofing compound was applied to the floor and walls to protect the subgrade from moisture changes. A clay material was compacted into this enclosure to a depth of 4 ft. Properties of the clay subgrade are given in Table 1. The modulus of subgrade reaction, k, is given in Table 5. It will be shown later that the average radius of relative stiffness for the 16 test slabs was 7.3 in. Therefore the subgrade depth was 6.6 times the radius of relative stiffness, and behavior should approximate a subgrade of infinite depth. The radius of relative stiffness, L, is a ratio of the stiffness of the slab to the stiffness of the subgrade (Eq. 3).

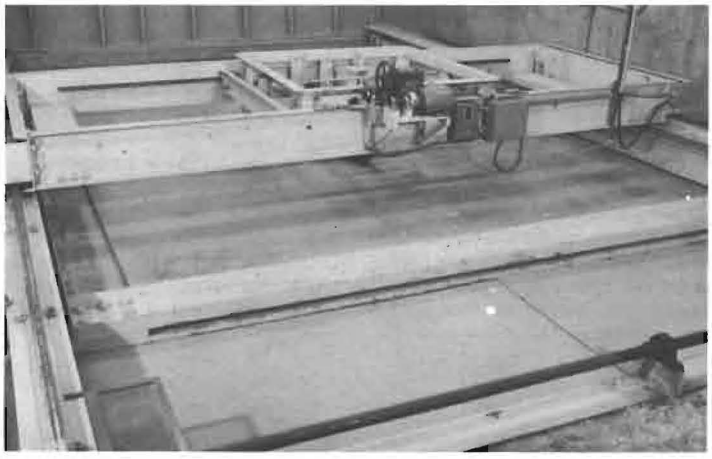

Figure 1. Test area and moving load apparatus.

TABLE 1

SUBGRADE PROPERTIES

Property	Particle Size (mm)	Percent	PCF
Material			
Gravel	76.2 -2.0	0	–
Coarse sand	2.0 -0.42	6	–
Fine sand	0.42 -0.074	8	–
Silt	0.074-0.005	48	–
Clay	smaller than 0.005	38	–
Liquid limit		36	–
Plasticity index		19	–
Maximum dry density (AASHO standard)		–	112
Optimum moisture		16	–

TABLE 2

SUBBASE PROPERTIES

Property	Particle Size (mm)	Percent	PCF
Granular Material			
Gravel	76.2 -2.0	46	–
Coarse sand	2.0 -0.42	24	–
Fine sand	0.42 -0.074	17	–
Silt	0.074-0.005	10	–
Clay	smaller than 0.005	3	–
Plasticity index		0	–
Maximum dry density (AASHO standard)		–	141
Optimum moisture		7	–
Cement-Treated Material			
Gravel	76.2 -2.0	27	–
Coarse sand	2.0 -0.42	23	–
Fine sand	0.42 -0.074	32	–
Silt	0.074-0.005	16	–
Clay	smaller than 0.005	2	–
Plasticity index		0	–
Maximum dry density (AASHO standard)		–	125
Optimum moisture		10	–
Cement content		5.5	–

Thirteen of the test slabs were cast on the clay subgrade without a subbase layer. The top surface of the clay was carefully finished to grade with a metal screed to obtain a level casting surface for uniform slab depth. After leveling, the subgrade was covered with two sheets of 4-mil thick polyethylene to retain moisture in the clay subgrade and to reduce stresses resulting from restraint to horizontal slab movement. The clay subgrade was removed to a depth of about 1 ft after each test and the soil was pulverized, reworked to optimum, and recompacted.

A 6-in. granular subbase was used under two of the test slabs, and a 6-in. cement-treated subbase was used under another. The properties of these subbases are given in Table 2. The modulus of subgrade reaction, k, is given in Table 5. For these tests the top 6 in. of clay subgrade was removed and replaced with subbase material. Polyethylene sheets were placed between the subbase and the concrete.

Prestressing

Test slabs were prestressed by the pretensioning method, i.e., the wires were tensioned prior to placing the concrete. After the concrete had attained sufficient strength,

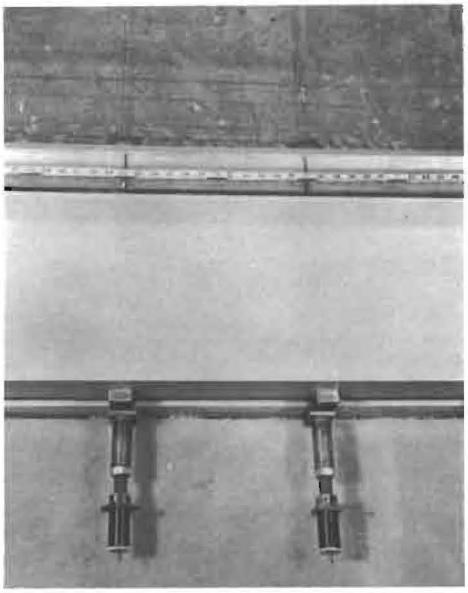

Figure 2. Devices used for tensioning the steel wires.

the wires were released and stress was transferred to the concrete through bond.

Uncoated, stress-relieved No. 12 steel wire was used for applying prestress at the mid-depth of the slabs. Wires in one direction alternated above and below those extending at right angles. The wire diameter was 0.1055 in., area 0.00875 sq. in., modulus of elasticity 27, 600, 000 psi, and ultimate strength 260, 000 psi.

The reaction frame used for tensioning the wires had inside dimensions of 14 by 17 ft. Each side of the frame was formed by a pair of 15-in. steel channels between which the wires were inserted. Bolted moment connections were used at the frame corners. Concrete beams resting on the clay subgrade supported the reaction frame in a horizontal plane at the proper elevation for tensioning the wires at slab mid-depth.

Each prestressing wire was tensioned individually by the extension of a telescoping threaded spacer placed between the wire anchor and the reaction frame (Fig. 2). The force in the wire was measured by a transducer (4) placed between the wire anchor and the reaction frame at the side opposite the spacer. After tensioning the wires, a minimum of one day was allowed before casting the concrete slab. The force in each wire was checked and, if necessary, adjusted to the selected magnitude prior to casting.

To insure full prestress near the slab edges, a 1-in. split steel cube was fastened to each wire at the point where the wire entered the steel side forms. The two halves of the cube were grooved slightly undersize for the wire used and were clamped on the wire by countersunk machine screws.

Casting of Concrete

The cement factor of the concrete was 7.0 sk/cu yd; water-cement ratio was 0.52 by weight, and the sand-aggregate ratio was 0.59 by weight. Type 3 cement was used to obtain a high early strength, and the maximum size of gravel aggregate was $\frac{3}{8}$ in. The slump averaged 4.7 in. and vinsol resin was added to provide an average air content of 6.9 percent. Concrete was compacted with a vibrating screed.

After casting, each slab was covered with polyethylene sheeting. The next day, approximately 16 hours later, the sheeting was removed and the top slab surface was coated with a curing compound to reduce moisture losses and thereby minimize curling. Prestressing wires were released after the concrete had cured for 7 days.

Beam specimens 1 by 4 by 22 in. were made at the time of casting from samples of concrete placed in the center portion of each test slab. The beams were cured in a 70 F, 100 percent relative humidity room until tested in flexure with third-point loading on a span of 12 in. It was usually possible to obtain two flexural tests from each beam. A minimum of nine beams was tested for each slab, including three tested when repetitive slab loading was started and three when each failure occurred. Repetitive load tests were started 12 to 14 days after casting. Duration of each test depended on the number of loadings necessary to cause failure and averaged 13 calendar days for all slabs. During the test period, there was relatively little change in the flexural strength of each slab; average values are given in Table 3.

TABLE 3
CONCRETE FLEXURAL STRENGTH

Slab No.	Modulus of Rupture (psi)	Slab No.	Modulus of Rupture (psi)
1	970	9	966
2	880	10	957
3	882	11	970
4	897	12	952
5	952	13	930
6	905	14	963
7	890	15	936
8	916	16	927

A limited number of beams were instrumented with two SR-4 type A9-4 (2-in. length) strain gages on the bottom surface between the third-point loads. Strain measurements during flexural testing of these beams indicated that the average modulus of elasticity for the test slabs was 4, 100, 000 psi.

Load Apparatus

A special load apparatus was constructed for applying repetitive moving loads to the prestressed concrete test slabs. The load apparatus was not designed to simulate traffic operations but rather to develop a random pattern of bottom surface cracks at the interior of each slab. Loads were applied through a single wheel traveling in a number of wheel paths over an interior area 32 in. wide (including the width of the wheel) by 98 in. long. The distances between the loading area and the longitudinal and transverse edges of the 12 by 16-ft slabs were 56 and 47 in. respectively. These edge distances were 7.7 and 6.4 times the average radius of relative stiffness of the test slabs, i.e., sufficient for load behavior to be similar to a slab of infinite surface area.

The equipment used to apply repetitive moving loads is shown in Figure 1. Load was applied through a 16-in. diameter wheel with a 4-in. wide solid rubber tire. The tire had longitudinal and transverse measurements scaled to represent the prototype. The contact area of the tire increased with increasing load as shown in Figure 3.

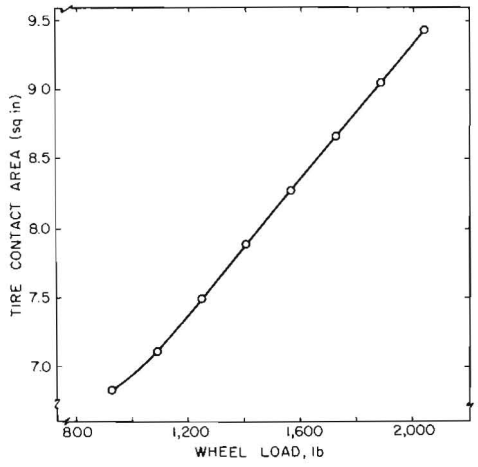

Figure 3. Contact area of solid rubber tire.

The paths traveled by the load wheel during the repetitive moving load tests are shown in Figure 4. Starting at location A, the wheel traveled 98 in. in a longitudinal path to location B. After returning in the same wheelpath to location A, the wheel was driven transversely a distance of 2 in. or half the width of the tire to a second longitudinal wheelpath. After returning to location C, the wheel was again driven transversely a distance of 2 in. to a third wheelpath. During each transverse movement of 2 in. the wheel traveled approximately 10 in. longitudinally. After traveling in 15 longitudinal wheelpaths or a total of 28 in. transversely to location D, the direction of transverse travel was reversed.

The Corps of Engineers (5) defines a load coverage as a sufficient number of vehicle operations or passes to produce

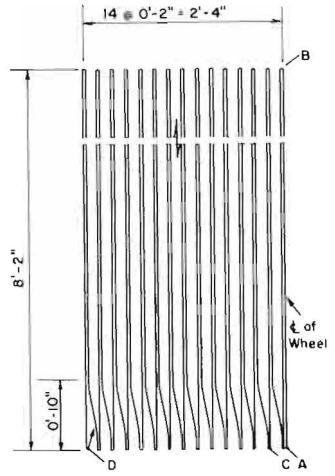

Figure 4. Wheelpaths during load testing.

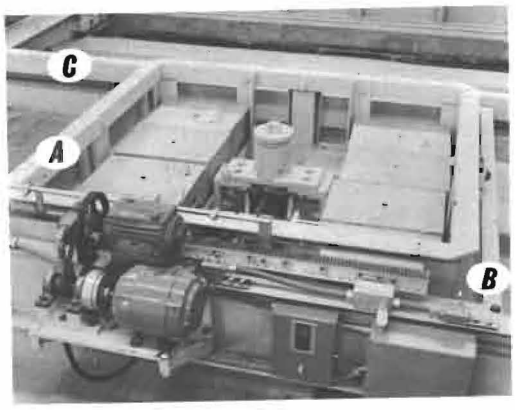

Figure 5. Load box.

statistically one application of the design loading over the entire traffic area. By this definition, 4 load coverages were applied each time the wheel traveled 28 in. transversely or from location A to D. The average wheel speed was 1.68 ft/sec and 106 coverages were applied per hour. Because this rate of loading is greater than that normally encountered on highway and airfield pavements, the data represent conditions more severe than those encountered in actual pavement service.

The load wheel was mounted in the center of a load box. To reduce transverse thrust on the test slabs when the wheel turned to change wheelpaths, the wheel was mounted as a caster with a swivel bearing. A spring mechanism was used to prevent the wheel from rotating 180 degrees on each return trip, as for example, from location B to A.

The load box, as represented by frame A in Figure 5, was made of steel angles welded together to form a frame 4 ft 5 in. by 4 ft 1 in. by 1 ft 5 in. deep. A pair of roller bearings that operated within a vertical channel at the center of each side of the load box enabled it to move freely in the vertical direction within frame B. The desired wheel load was obtained by placing concrete weights inside the load box.

Frame B was designed to move transversely within frame C by means of roller bearings that traveled on transverse bars bolted to the inside of the inside of the span beams of frame A. Power for driving frame B in the transverse direction was supplied by a ½-hp electric motor mounted on frame C. As shown in Figure 5, the motor acted through an electric clutch to drive a pinion gear over a rack mounted on frame B. Length of transverse travel was controlled by a number of stops contacting an electrical switch that regulated current to the clutch.

Frame C had a transverse span of 18 ft and a longitudinal length of 5 ft. A flanged crane wheel mounted near each corner traveled on longitudinal rails that were supported by steel beams independent of the subgrade and prestressing frame. Power for driving frame C in the longitudinal direction was supplied by a 5-hp electric motor. Operating through a gear reducer to obtain proper speed, the motor rotated a transverse steel shaft located near one end of the rails. Two steel drums were mounted on the shaft, one near each end between the flanges of the rail support beams. Each drum pulled a steel cable that traveled around a fixed pulley at the opposite end of the rails. Frame C was attached to the two cables to obtain longitudinal motion when the electric motor was operating. Length of longitudinal travel was controlled by an electrical switch that was activated when the load device passed either of two selected rail locations. This switch disconnected current and applied an electric brake to the motor. By regulating the electric current to the brake, the load device could be smoothly decelerated. An electrical switch on the motor shaft was used to determine when the load device had stopped and to start travel in the opposite longitudinal direction.

Figure 6. Failure in top surface of slab 2.

Instrumentation

Slab deflections were measured by a resistance bridge deflectometer (6) buried in the clay subgrade 2 ft below the test slabs. The deflectometer was restrained from vertical movement by a steel rod that extended between the deflectometer casing and the concrete slab under the clay subgrade. A second steel rod extended upward from the measurement control pin of the deflectometer to a fitting cast in the slab. An electrical connection between the deflectometer and chart recording equipment enabled deflections to be continuously measured as the load wheel approached and passed over the deflectometer location.

Strains were measured by pairs of SR-4 type A9-4 (2-in. long) strain gages cemented to the top surface of the test slabs, one in the longitudinal and one in the transverse direction at the same location. Strains were also recorded continuously as the load wheel approached and passed over the gages.

TEST RESULTS

Data are reported for load tests on 16 prestressed slabs. The spacing between prestressing wires, amount of tensile force in each wire, and resultant concrete prestress of each test slab are given in Table 4.

Moving loads were applied repeatedly to 15 of the test slabs until failure occurred. Wheel loads and number of coverages at failure are given in Table 5. Failure was characterized by a crumbling of the concrete in the top surface of the slab within a circular area approximately 12 in. in diameter (Fig. 6). These failures occurred very suddenly. Only a few additional load coverages were necessary for the top surface of the slab to deteriorate from the initial cracked condition to the failed condition shown. Failures occurred at random locations within the loaded areas. For most slabs, a thin steel plate was placed over the failed area and repetitive loading was continued until a second failure occurred. A bottom surface view of one of the slabs after a failure had occurred is shown in Figure 7. This photograph shows only a cut out interior portion of the slab where the moving loads were applied. Visual bottom surface cracks were indicated by black ink. Loose concrete was removed at the failure location to expose the prestressing wires. There were no wire failures during any of the load tests. After load testing

TABLE 4

REINFORCEMENT AND PRESTRESS PROPERTIES OF TEST SLABS

Slab No.	Wire Spacing (in.)		Wire Tensile Force (lb)	Concrete Prestress (psi)	
	Long.	Trans.		Long.	Trans.
1-8	12	12	1200	100	100
9	36	36	1200	33	33
10	None	None	0	0	0
11	12	12	140	12	12
12	12	0	1200	100	0
13-16	12	12	1200	100	100

TABLE 5

PROPERTIES OF TEST SLABS

Slab No.	Wheel Load (lb)	Coverages at Failure	h (in.)	k (pci)	L (in.)	a (in.)	α	m_c (in. lb./in.)
1	1730	5730	1.02	70	8.53	1.66	0.195	185
		7270	1.02	70	8.53	1.66	0.195	185
2	1571	2444	1.00	80	8.13	1.62	0.199	165
		3010	1.01	80	8.19	1.62	0.198	168
3	1571	2116	1.01	100	7.75	1.62	0.209	167
		2780	1.02	100	7.80	1.62	0.208	171
4	1410	2098	0.97	100	7.52	1.58	0.210	156
		3816	0.98	100	7.58	1.58	0.208	159
5	1410	25060	1.02	105	7.71	1.58	0.205	182
6	1730	330	0.96	110	7.28	1.66	0.228	155
		342	0.95	110	7.23	1.66	0.230	152
7	1571	472	0.92	120	6.90	1.62	0.235	140
		946	0.93	120	6.96	1.62	0.233	143
8	1571	6160	1.00	120	7.35	1.62	0.220	169
		7700	0.99	120	7.29	1.62	0.222	166
9	1571	7506	1.01	120	7.40	1.62	0.219	170
		8538	1.02	120	7.46	1.62	0.217	173
10	1571	860	1.01	120	7.40	1.62	0.219	163
11	1571	1676	1.02	120	7.46	1.62	0.217	170
12	1571	3226	1.00	120	7.35	1.62	0.220	159
13	Static Load Test		1.02	125	7.38	2.00	0.271	179
14	1730	18500	1.01	170	6.78	1.66	0.245	181
	Static Load Test		1.03	170	6.91	2.00	0.289	188
15	2049	1022	0.97	180	6.49	1.72	0.265	163
		1164	0.98	180	6.53	1.72	0.263	166
16	2206	0 to 14500[a]	1.00	320	5.75	1.76	0.306	171
	3478	14500 to 33700[a]	1.00	320	5.75	1.99	0.246	171

[a]Slab 16 did not fail.

was completed, slab thickness at each failed area was measured with a vernier caliper. Average thicknesses are given in Table 5.

A previous theoretical analysis (1) of prestressed concrete pavements indicated that strength is a function of α and m_c, where

$$\alpha = \frac{a}{L} \tag{1}$$

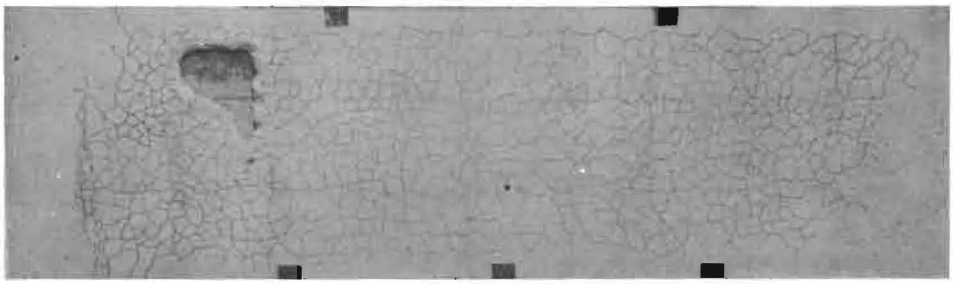

Figure 7. Crack pattern in bottom surface of slab 5.

and

$$m_c = \frac{\sigma_c h^2}{6} \tag{2}$$

in which

L = radius of relative stiffness (in.), i.e.,

$$L = \sqrt[4]{\frac{E h^3}{12 (1 - \mu^2) k}} \tag{3}$$

a = radius of loaded area (in.),
E = concrete elastic modulus (psi),
μ = Poisson's ratio,
h = slab thickness (in.),
k = subgrade modulus (pci),
σ_c = cracking stress (psi) = modulus of rupture plus prestress, and
m_c = cracking moment (in.lb/in. of width).

Computed m_c and α-values for each slab are given in Table 5. The radius of the loaded area, a, used to compute α-values was the radius of a circle having an area equal to that shown in Figure 3 for the loaded tire at the test load. The radius of relative stiffness, L, was computed using the measured value of 4,100,000 psi for the modulus of elasticity, E, and an assumed value of 0.15 for Poisson's ratio. The subgrade modulus, k, was determined with a 30-in. diameter plate at 0.05 in. deflection. The k-value given in Table 5 is the average of the values determined prior to the construction and after the testing of each slab. When computing m_c-values, cracking stresses were assumed to be equal to the summations of the modulus of rupture values given in Table 3 and the prestress values given in Table 4.

Analyses

To analyze the test data given in Table 5 and develop a design method for prestressed pavements, it is necessary to relate m_c and α-values with wheel loads and coverages causing failures. This may be done by using the m_c and α-values to compute either the bottom or the top surface cracking load of each slab, then establishing a relationship between the ratio of such cracking load to applied wheel load and the coverages causing failure.

Bottom Cracking

The following equation, based on Westergaard's (7) theoretical analysis for loads applied in the interior of the area of a panel, can be used to compute the bottom cracking load, P_c:

$$\left.\begin{matrix}\sigma_x \\ \sigma_y\end{matrix}\right\} = \frac{P}{h^2}\left[0.275 (1 + \mu) \log_{10} \frac{Eh^3}{k\left(\frac{a + b}{2}\right)^4} \mp 0.239 (1 - \mu) \frac{a - b}{a + b}\right] \tag{4}$$

where σ_x and σ_y = principal tensile stresses in the directions of x and y at the bottom of the slab under the center of the load, and a and b = semiaxes of an ellipse representing the footprint of a tire. For a circular loading area where a = b and letting $\mu = 0.15$, $L^4 = \frac{Eh^3}{12(1 - \mu^2)k}$, $\alpha = \frac{a}{L}$, and $m_c = \frac{\sigma_x h^2}{6}$, Eq. 4 becomes:

$$P_c = \frac{m_c}{0.0527\left(4 \log_{10} \frac{1}{\alpha} + 1.069\right)} \tag{5}$$

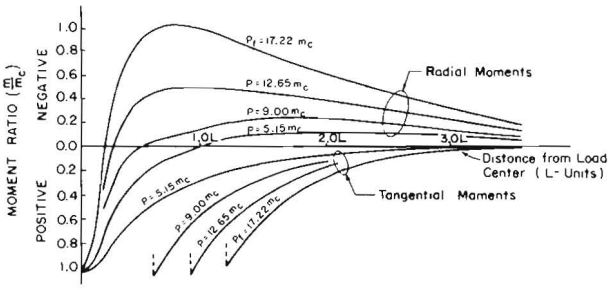

Figure 8. Radial and tangential moment curves—PCA theoretical method for $\alpha = 0.2$.

Top Cracking

The top surface cracking load of a prestressed pavement may be computed by the PCA theoretical method (1). This method is limited to a load applied at an interior position of a slab supported by a dense liquid foundation and prestressed equally in the longitudinal and transverse directions. By use of this method, radial and tangential moment diagrams were developed for loads greater than those causing bottom surface cracking, i.e., beyond conditions to which the elastic theory is applicable. Example moment diagrams for $\alpha = 0.2$ are shown in Figure 8. Bottom surface cracks begin to form under the load when the positive moment, m, equals the cracking moment, m_c, or when $m/m_c = 1$. A small increase in load beyond that initiating bottom cracking will cause these cracks to extend radially from the center of the load. As additional load is applied, there is an increase in the positive tangential moment and negative radial moment. The bottom surface radial cracks become longer, and the point of zero radial moment moves nearer the center of loading. At a load, P_F, equal to 17.22 times the cracking moment, m_c, the negative radial moment equals the cracking moment and a circular crack occurs in the top surface of the slab. Other top surface cracking loads predicted by the PCA method for α-values varying from 0.1 to 0.5 may be determined from the diagram shown in Figure 9.

Another method for computing top surface cracking loads is that used by the Corps of Engineers. Based on the results of previous static load tests on Hydrocal model slabs 16.6 in. square by 0.20 in. thick and supported on a 12-in. thick layer of natural rubber, the following empirical equation was developed (8):

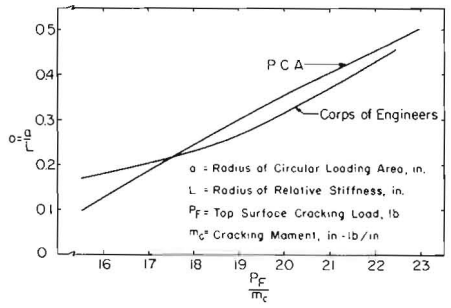

Figure 9. Top surface cracking loads for prestressed concrete pavements.

$$P_F = \frac{h^2 (R + R_P)}{6\left[C\frac{M_o}{P_o} - \frac{M_R}{P_o}\right]} \qquad (6)$$

where

P_F = top surface cracking load (lb),
h = slab thickness (in.),
R = flexural strength of the concrete (psi),
R_P = concrete prestress (psi),
C = radial moment correction factor,
M_o/P_o = moment coefficient under center of loaded area, and
M_R/P_o = moment coefficient at point of negative moment cracking.

TABLE 6

DESIGN FACTORS BASED ON TOP CRACKING LOADS

Slab No.	Wheel Load (lb) P	Coverages at Failure	Bottom Cracking Load (lb) P_c	Top Cracking Load (lb) P_F			Fatigue Factors	
				PCA	C of E	Average	$\frac{P}{P_c}$	$\frac{P_F}{P}$
1	1730	5730	898	3170	3080	3125	1.93	1.81
		7270	898	3170	3080	3125	1.93	1.81
2	1571	2444	809	2800	2730	2765	1.94	1.76
		3010	824	2860	2790	2825	1.91	1.80
3	1571	2116	835	2900	2870	2885	1.88	1.84
		2780	855	2950	2910	2930	1.84	1.87
4	1410	2098	784	2730	2700	2715	1.80	1.93
		3816	795	2780	2740	2760	1.77	1.96
5	1410	25060	905	3150	3100	3125	1.56	2.22
6	1730	330	807	2720	2760	2740	2.14	1.58
		342	796	2680	2720	2700	2.17	1.56
7	1571	472	741	2500	2540	2520	2.12	1.60
		946	753	2540	2580	2560	2.09	1.63
8	1571	6160	867	2960	2960	2960	1.81	1.88
		7700	856	2920	2930	2925	1.84	1.86
9	1571	7506	870	2990	2990	2990	1.81	1.90
		8538	881	3060	3000	3030	1.78	1.93
10	1571	860	834	2920	2930	2925	1.88	1.86
11	1571	1676	866	2980	2980	2980	1.81	1.90
12	1571	3226	815	2940	2940	2940	1.93	1.87
13	Static Load Test		1017	3310	3420	3365	—	—
14	1730	18500	978	3260	3340	3300	1.77	1.91
	Static Load Test		1106	3530	3660	3595	—	—
15	2049	1022	916	2980	3080	3030	2.24	1.48
		1164	927	3040	3140	3090	2.21	1.51
16	2206	—[a]	1036	3270	3390	3330	2.13	1.51
	3478	—[a]	1118	3390	3510	3450	3.11	0.99

[a]Slab 16 did not fail.

In using this equation, values of C, M_O/P_O, and M_R/P_O must be obtained from appropriate curves (8). These values are plotted as functions of either A/L^2 or a/L where A is the area of the loaded area, a is the radius of the loaded area, and L is the radius of relative stiffness, so that it is possible to develop a relationship between P_F/m_c and a/L where m_c is equal to $h^2 (R + R_P)/6$. The resultant curve for circular loading areas is compared to the PCA method in Figure 9. It is seen that the two methods are in fair agreement.

Slabs on Clay Subgrade

Data are presented from tests on the nine slabs cast on a clay subgrade and prestressed to 100 psi in both longitudinal and transverse directions. Comparisons will later be made with the four slabs that had reduced amounts of prestress and with the three slabs cast on granular and cement-treated subbases.

Using the m_c and α-values given in Table 5, bottom surface cracking loads were computed by Westergaard's Eq. 5, and top surface cracking loads were computed by both the PCA and Corps of Engineers method using Figure 9. Top cracking loads by the two methods were nearly equal for each slab failure, and average values were used to determine ratios of computed top surface cracking loads divided by repetitive moving wheel loads. Also, ratios of repetitive moving loads divided by bottom surface cracking loads were determined. These ratios are given in Table 6 and in this report are defined as fatigue factors. Fatigue factors are plotted in Figure 10A and 10B vs the number of load coverages causing failure.

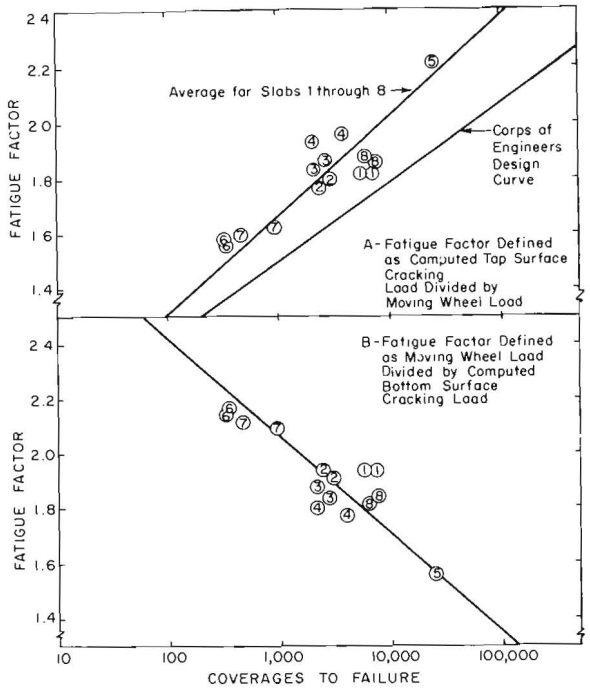

Figure 10. Fatigue relationships for prestressed concrete pavements.

The results of these tests may be compared with data from a similar moving load test program conducted by the Corps of Engineers (5). The essential differences between these two programs were as follows:

Characteristic	Corps of Engineers	PCA
Casting Technique	Precast	Cast in place
Prestressing: Method	Pretensioned	Pretensioned
Amount	250 psi	100 psi
Size of Slab: Length	15 ft	16 ft
Width	6 ft	12 ft
Thickness	1 in.	1 in.
Size of Loaded Area: Length	120 in.	98 in.
Width	24 in.	32 in.
Avg. Conc. Mod. of Rupt.	905 psi	914 psi
Avg. Conc. Elas. Mod.	4,500,000 psi	4,100,000 psi
Avg. Subgrade Modulus	65 pci	105 pci

In analyzing their data, the Corps of Engineers plotted a curve that related a design factor for repetitive loading to the number of load coverages causing failure. Their design factor was defined as the computed top surface cracking load for a single application divided by the repetitive moving wheel load. This curve is shown on the appropriate diagram in Figure 10A. For a given fatigue ratio, it indicates a greater number of coverages at failure than the PCA curve.

TABLE 7

CRACKING LOADS FROM PREVIOUS STATIC LOAD TEST PROGRAM (2)

Slab No.	α	m_c (in. lb./in.)	Measured Cracking Loads (lb)		Theoretical Cracking Loads (lb)	
			Bottom	Top	Bottom	Top
1	0.315	155	880	4140	900	2950
2	0.525	155	1220	4820	1270	3570
3	0.315	130	850	4180	780	2470

In designing a prestressed pavement using the data shown in Figure 10A and 10B, the fatigue factor may be based on either the top or bottom cracking load. However, it will be shown that top cracking loads measured during static load tests on prestressed pavements are usually greater than those predicted by either the PCA or Corps of Engineers method, whereas measured bottom cracking loads can be accurately predicted by elastic theory analysis. Also, to measure the strength of an in-service prestressed pavement, the bottom cracking load can be more readily determined by a static load test than the top cracking load, which would result in permanent damage to the pavement. Therefore, in analyzing the remaining data in this report, fatigue factors will be based only on the bottom surface cracking loads.

Static Load Tests

A previously reported (2) program of static load tests on prestressed concrete slabs indicated that the PCA theoretical method (1) provided conservative top surface cracking loads. In that program, reduced scale slabs, 8 ft by 8 ft by 1 in. thick, were loaded through centrally located circular plates while supported on a coil spring subgrade. A summary of bottom and top surface cracking loads from these tests is given in Table 7. Measured and theoretical bottom cracking loads were in agreement but measured top cracking loads were an average of 46 percent greater than theoretical values.

The theory assumed that the moment-curvature relationship could be represented by two straight lines, i.e., an elastic portion with a constant slope, followed by a plastic portion where curvature increased at a constant maximum moment equal to the cracking moment. The experimental slabs did not react in accordance with this assumption; moments greater than the initial cracking moment occurred after bottom surface cracking. This was the major reason that experimental top cracking loads were greater than those predicted theoretically.

The theory also assumed that bottom surface cracks extend radially from the center of the loaded area as load is increased. This assumption was confirmed by experimental data for static loading. However, under traffic load conditions the radial cracking is altered, and the assumed theoretical moment-curvature relationship may possibly be more appropriate. To study the effects of a random pattern of bottom surface cracks on load behavior, static load tests were conducted on slabs 13 and 14. The only test conducted on slab 13 was with a static load, so that the slab was in an uncracked condition prior to loading. The static load test on slab 14 was made after one failure had occurred from applications of repetitive moving load. The static load was applied through a 2-in. radius steel plate in 500-lb increments until top surface cracking occurred. A $\frac{1}{2}$-in. thick rubber pad was placed between the plate and slab to aid in obtaining uniform load distribution. Both slabs were instrumented to measure maximum deflection at the load as well as radial and tangential strains at the load and at locations 7, 10, and 13 in. from the load.

Stresses were computed from the measured strains using

$$\sigma_r = \frac{E}{1 - \mu^2} (\epsilon_r + \mu \epsilon_t) \qquad (7)$$

$$\sigma_t = \frac{E}{1 - \mu^2} (\epsilon_t + \mu \epsilon_r) \quad (8)$$

in which

σ_r = radial stress,
σ_t = tangential stress,
ϵ_r = measured radial strain,
ϵ_t = measured tangential strain,
E = concrete modulus of elasticity, 4,100,000 psi, and
μ = Poisson's ratio, assumed 0.15.

Maximum top surface compressive stresses resulting from positive moment at the center of the loaded area and maximum top surface tensile stresses resulting from negative radial moment beyond the point of contraflexure were determined for each load increment. These stresses together with maximum deflections are plotted in Figures 11 and 12.

Experimental top surface compressive stresses at the load center were used to determine the bottom surface cracking load for slab 13. Assuming that, before cracking occurred, top surface compressive stresses equaled bottom surface tensile stresses and that the cracking stress was 1030 psi, the experimental data indicated a bottom cracking load of 960 lb for slab 13. At this load, there was a slight change in the slope of the experimental load-stress curve. In comparison, the theoretical bottom cracking load as determined by Westergaard's analysis using Eq. 5 was 1018 lb for slab 13. Before bottom cracking, there was good agreement between experimental and theoretical stresses for slab 13; however, for slab 14 experimental stresses were approximately 40 percent greater than theoretical stresses. This expected difference was due to the extensive bottom surface cracking that had already occurred in slab 14 during 18,500 coverages of a 1730 lb moving wheel load.

For the PCA theoretical method, curves shown in Figure 13 indicate the relationship between maximum theoretical deflection, y, subgrade modulus, k, radius of relative stiffness, L, cracking moment m_c, radius of loaded area, a, and applied load, P. The curves in Figure 14 indicate the relationship between maximum theoretical negative radial moment, m_n, radius of relative stiffness, L, cracking moment, m_c, radius of loaded area, a, and applied load, P. Using these curves and the slab properties given in Table 5, maximum theoretical deflections and maximum theoretical top surface tensile stresses resulting from negative radial moments were determined for loads less than theoretical top cracking loads. Theoretical curves are compared with experimental data in Figures 11 and 12.

Experimental and theoretical deflections were in good agreement, but experimental top surface tensile stresses were generally greater than theoretical values. As a result, experimental top surface cracking loads were 4300 and 5000 lb for slabs 13 and 14, respectively, or an average of 36 percent greater than theoretical top cracking loads of 3310 and 3530 lb. Also, measured radii of the top surface cracks were an average of 10 in. compared with a theoretical average of 7 in. There did not appear to be any reduction in either top surface tensile stresses or top cracking loads as a result of the bottom surface cracking that occurred in slab 14 during repetitive moving load testing prior to the static test.

From these data it was concluded that, by existing methods of analysis for prestressed concrete pavement, bottom cracking loads can be more accurately predicted than top cracking loads. Therefore, for a prestressed pavement it appears more rational to base a fatigue factor for traffic load conditions on the bottom cracking load.

Influence of Prestress

The influence of magnitude and distribution of prestress on the load behavior of prestressed concrete pavements was studied by reducing the prestress in four of the test slabs. As shown in Table 4, all slabs except 9, 10, 11, and 12 had a concrete prestress of 100 psi in both longitudinal and transverse directions. In slab 9, the spacing

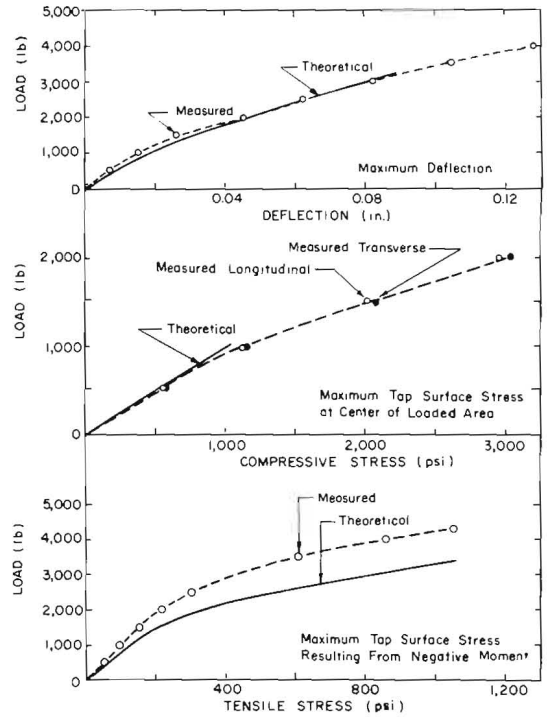

Figure 11. Static load test data—slab 13 (no prior loading).

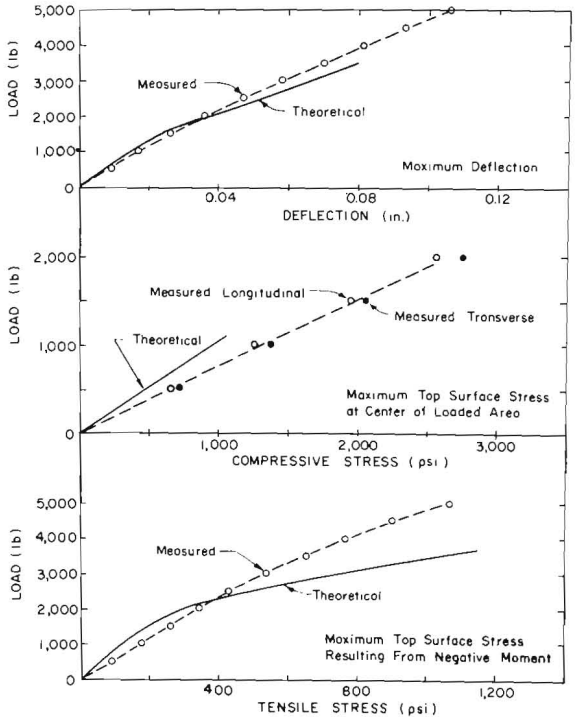

Figure 12. Static load test data—slab 14 (after repeated loading).

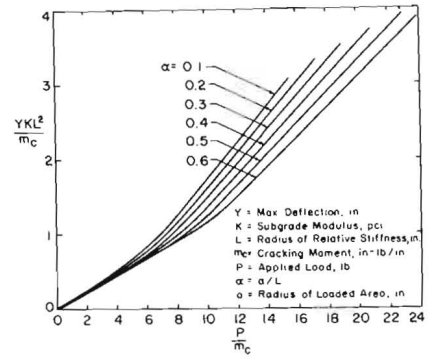

Figure 13. Relationship established by PCA theoretical analysis for deflections.

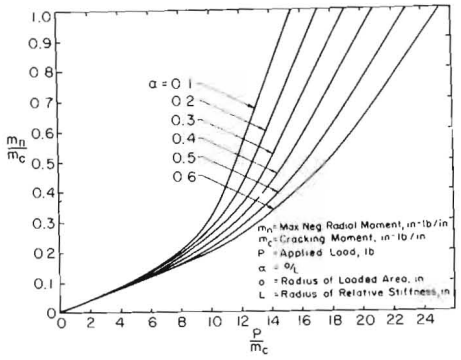

Figure 14. Relationship established by PCA theoretical analysis for moments.

of the steel wires was tripled from 12 to 36 in.; with a force of 1200 lb on each wire, the resulting prestress was reduced from 100 to 33 psi. Slab 10 did not contain any steel wires and was therefore neither reinforced nor prestressed. In slab 11, a spacing of 12 in. was used for the steel wires. However, the force on each wire was reduced to that needed for straightening the wires. This force was 140 lb on each wire and resultant prestress was 12 psi. Slab 12 did not contain any transverse steel wires; longitudinal wires were spaced 12 in. apart and had a force of 1200 lb on each wire, resulting in a longitudinal prestress of 100 psi.

Slabs 9 to 12 were tested with a 1571-lb repetitive moving wheel load until at least one slab failure occurred. Slabs 10 and 12 did not fail in the same manner as the other slabs, i.e., with a sudden crumbling of the concrete in the top surface of the slab. Slab 10 with neither reinforcement nor prestress showed distress earlier than the other test slabs, and top surface cracking developed over the entire loaded area after only a few load coverages, although it required 860 coverages before failure. Slab 12, with only longitudinal prestress, developed a longitudinal crack over each wire in the loaded area after a few hundred load coverages, although 3226 coverages were required before failure. Therefore, it was concluded that two-way prestress is required to avoid top surface cracking when relatively few moving loads greater than those causing bottom surface cracking are applied repeatedly at interior locations.

Fatigue factors were determined for slabs 9 and 11 by dividing the 1571-lb wheel load by the bottom cracking load computed from Westergaard's equation (Eq. 5). These fatigue factors are given in Table 6 and are plotted in Figure 15 as a function of the number of load coverages causing failure. Data from slab 9 (33 psi, 2-way prestress) were in better agreement than slab 11 (12 psi, 2-way prestress) with the curve determined from tests on slabs 1 through 8 (100 psi, 2-way prestress). Because of this it was considered that a prestress of 33 psi is approximately the minimum required for prestressed concrete pavements to support repeated moving loads greater than those causing bottom surface cracking.

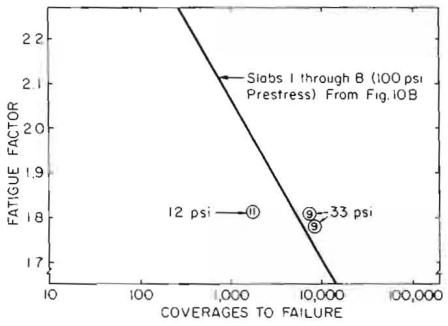

Figure 15. Effect of magnitude of prestress on fatigue.

Influence of Foundation Strength

The influence of foundation strength on the load behavior of prestressed concrete

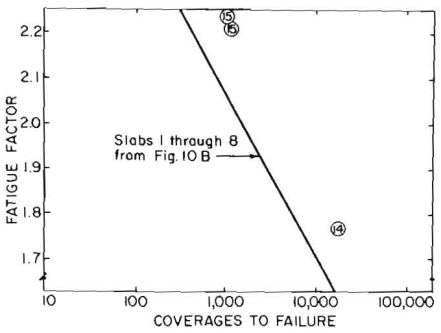

Figure 16. Effect of foundation strength on fatigue.

pavements was studied by casting three of the test slabs on 6-in. thick subbases. A granular subbase was used under slabs 14 and 15, and a cement-treated subbase was used under slab 16.

Slabs 14 and 15 failed in the same manner as slabs 1 through 8, i.e., with a sudden crumbling of the concrete in the top surface of the slab. Fatigue factors were determined by dividing the applied moving wheel load by the bottom cracking load computed from Westergaard's equation (Eq. 5). These fatigue factors are given in Table 6 and are plotted in Figure 16 as a function of the number of load coverages causing failure. Results are compared with the curve determined for slabs 1 through 8. Each of these slabs was prestressed to 100 psi in both longitudinal and transverse directions. However, the average subgrade modulus of the clay subgrade under slabs 1 through 8 was 100 pci compared to the modulus of 175 pci for the granular subbase under slabs 14 and 15. As would be expected, the curve determined for slabs 1 through 8 predicted a conservative number of load coverages for slabs 14 and 15 with the stronger foundation.

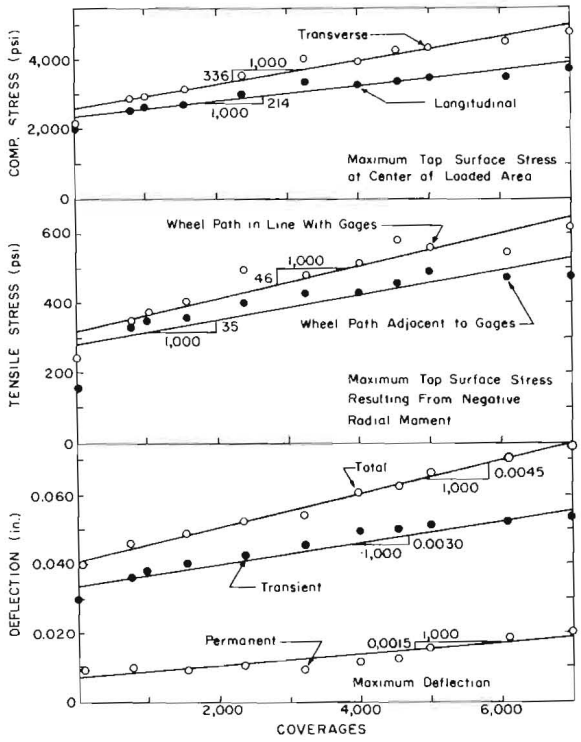

Figure 17. Typical stress and deflection values—slab 8.

Slab 16, cast on a cement-treated subbase with a modulus of 320 pci, did not fail after 14, 500 coverages of a 2206-lb load. The load was then increased to 3478 lb, or approximately that predicted by the PCA theoretical method as the top surface cracking load for a single, static application. After 19, 200 additional coverages, failure of the slab had not occurred and the test was discontinued. This demonstrates the advantage of a high-strength subbase under thin pavements. Stresses and deflections of slab 16 were much less than those predicted by theory. Measured strains at the load center indicated a bottom surface cracking load of 1570 lb as compared to the 1035-lb load predicted by Eq. 5. Therefore, the load behavior of slab 16 was not in agreement with Westergaard's theoretical analysis.

Strain and Deflection Data

Strain gages and deflectometers were connected to chart recording equipment to obtain continuous measurements as the load wheel approached and passed over their locations. At intervals of approximately 1000 moving load coverages on each slab, strains and deflections were continuously recorded as the load wheel traversed the entire loaded area. From these recordings, it was possible to determine (a) the maximum longitudinal and transverse compressive strain as the load wheel passed over the strain gages, (b) the maximum longitudinal tensile strain resulting from negative radial moment as the load wheel approached the strain gages, (c) the maximum transverse tensile strain resulting from negative radial moment as the load wheel passed the strain gages in an adjacent wheelpath, and (d) the maximum deflection as the load wheel passed over the deflectometer location. Stresses were computed from the measured strains using Eqs. 7 and 8.

Typical stress and deflection diagrams are shown in Figure 17. During the initial moving load coverage on slab 8, the top surface compressive stresses when the load wheel passed over the strain gages were 2000 and 2160 psi in the longitudinal and transverse directions respectively. These stresses were both greater than the theoretical value of 1880 psi computed by Westergaard's equation. Measured and theoretical values for the other test slabs are given in Table 8. As all slabs were loaded beyond elastic conditions, the measured values except for slab 16 were, as expected, greater than those computed by Westergaard's equations based on elastic theory. As previously discussed, the load behavior of slab 16 on the cement-treated subbase was not in agreement with Westergaard's theoretical analysis. Maximum top surface radial tensile stresses during the initial moving load coverage on slab 8 (Fig. 17) were 240 psi when the load wheel was in line with the strain gages and 156 psi when the load wheel was adjacent to the strain gages. These stresses were both less than the theoretical value of 246 psi computed by the PCA method using the relationships shown in Figure 14. Measured values for the other test slabs, as given in Table 8, were also generally less than the theoretical values with the exception of slab 10, which was unreinforced, and slab 12, which had only longitudinal prestress.

The initial measured deflection of slab 8 was 0.030 in., compared with a theoretical deflection of 0.037 in. computed by the PCA method using the relationships shown in Figure 13. Measured and theoretical deflections for the other test slabs are given in Table 8. As expected, measured moving load deflections were generally less than theoretical values based on static load conditions.

It can also be seen in Figure 17 that stresses and deflections increased with the number of load coverages. The average rate of increase was determined by computing the slope of the best-fit straight line for each set of data. For example, deflections of slab 8 increased at an average rate of 0.003 in. per 1000 load coverages until failure occurred. Rates of increase for the other test slabs are given in Table 8. These rates of increase were compared with fatigue factors computed by dividing the moving wheel load by the bottom surface cracking load of each slab. As shown in Figure 18, slabs tested at greater fatigue factors had generally greater rates of stress and deflection increases. It is also seen that the rates of increase for slabs 10 through 12 were much greater than those for slabs 1 through 9. Slab 10 was unreinforced, slab 11 had 12 psi, two-way prestress, and slab 12 had only longitudinal prestress, whereas slabs 1 through

TABLE 8

STRESSES AND DEFLECTIONS MEASURED DURING INITIAL COVERAGE OF MOVING LOAD

Slab No.	Wheel Load (lb)	Top Surface Compressive Stress at Load Center					Max. Top Surface Tensile Stress From Negative Radial Moment					Max. Transient Deflection		
		Measured (psi)		Theor. (psi)	Increase (psi/1000 cov.)		Measured (psi)		Theor. (psi)	Increase (psi/1000 cov.)		Measured (in.)	Theor. (in.)	Increase (in./1000 cov.)
		Long.	Trans.		Long.	Trans.	In Line	Adj.		In Line	Adj.			
1	1730	2500	2940	2050	282	226	244	147	260	10	48	0.051	0.053	0.008
2	1571	2050	2170	1910	534	723	206	210	240	319	188	0.051	0.046	0.012
3	1571	2970	3590	1830	1057	515	131	189	230	28	172	0.043	0.039	0.003
4	1410	2210	2450	1780	385	650	101	105	220	13	37	N. G.	0.037	N. G.
5	1410	1930	1800	1640	17	140	156	110	190	6	63	0.028	0.031	0.001
6	1730	2600	3160	2160	6140	4980	391	269	340	361	563	0.051	0.049	0.080
7	1571	2490	2420	2090	1712	1692	298	214	320	148	257	0.038	0.044	0.024
8	1571	2000	2160	1880	214	336	240	156	240	46	35	0.030	0.037	0.003
9	1571	2240	2980	1790	193	276	160	210	230	37	63	0.034	0.035	0.006
10	1571	2390	4030	1810	1990	2650	357	436	240	618	1240	0.036	0.037	0.022
11	1571	2100	1820	1780	1328	1930	260	198	230	511	295	0.029	0.035	0.014
12	1571	1960	1900	1840	858	3520	252	341	250	266	1300	0.031	0.038	0.011
13	Static Load Test													
14	1730	2080	2040	1880	84	68	134	227	260	11	15	0.029	0.033	0.001
15	2049	2940	2850	2310	1150	1700	332	357	430	122	207	0.044	0.045	0.025
16	2206	1560	1320	2110	14	19	101	88	410	2	11	0.016	0.034	0.004

N.G. = Deflectometer inoperable.

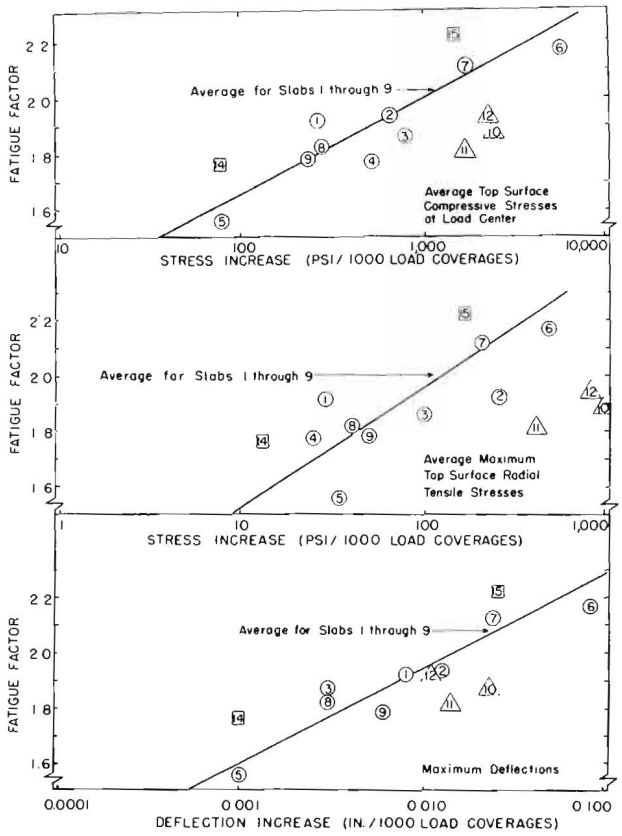

Figure 18. Effect of fatigue factor on rate of increase of slab stresses and deflections.

9 contained at least 33-psi, two-way prestress. In contrast, the rates of increase for slabs 14 and 15 were much less than those for slabs 1 through 9. These slabs were cast on a 6-in. thick granular subbase with an average k-value of 175 pci, whereas slabs 1 through 9 were cast on a clay subgrade with an average k-value of 100 pci.

Test data from all slabs were studied to determine the causes of prestressed concrete pavement failures. As shown in Table 8, none of the top surface tensile stresses resulting from negative radial moment was more than half the cracking stress during initial moving load applications. Therefore, slab failures were probably not caused by fatigue of the concrete in the top surface of the slab due to a repetition of radial tensile stresses. Rather, there appeared to be a progressive deterioration of the pavements caused by bottom surface cracks extending upward toward the top surface accompanied by increased deflections and a reduction in the concrete area needed to resist externally applied moments.

Relationship Between Model and Prototype

The model-size prestressed slabs used in this test program were purposely overloaded to obtain early failures. To indicate the degree of overloading, a comparison is made with a prototype prestressed concrete pavement. The following loading conditions and pavement properties are considered:

Load = 50, 000 lb applied repeatedly at interior locations,
Loaded area = 267 sq in.,
Slab thickness = 6 in.,
Concrete strength = 700 psi,
Minimum concrete prestress = 100 psi longitudinally and transversely,
Elastic modulus = 4, 000, 000 psi,
Poisson's ratio = 0.15, and
Subgrade modulus = 120 pci.

This prototype pavement has a radius of relative stiffness, L = 28.0 in., radius of loaded area, a = 9.2 in., α = a/L = 0.328, and cracking moment, m_c = 4800 in. lb/in. From Eq. 5, where $m_c = 0.0527\ P_c(4 \log_{10} 1/\alpha + 1.069)$, the bottom cracking load, P_c, equals 30,200 lb and the fatigue factor, P/P_c, equals 1.66. From the curve in Figure 10B, approximately 13,500 coverages can be applied before failure occurs. Maximum deflections for initial load applications can be determined from Figure 13, because deflections predicted by these curves were in good agreement with measured deflections. For P/m_c = 10.4 and α = 0.328, the deflection, y, equals 0.077 in.

In this comparison, it should be noted that the fatigue curve shown in Figure 10B is based on an ultimate failure caused by loads applied at interior locations. A safety factor should be included in a practical design method for prestressed concrete pavements.

SUMMARY

To obtain information on the fatigue characteristics of prestressed concrete pavements, 16 pretensioned, cast-in-place slabs were load tested. The slabs were purposely overloaded to cause failure under repeated loading. The results are summarized in the following:

1. Moving loads with magnitudes greater than those causing bottom surface cracking were applied repeatedly to an interior area of 15 of the test slabs until failure occurred. Failure was characterized by a crumbling of the concrete in the top surface of the slab. For slabs that had sufficient longitudinal and transverse prestress, failures occurred soon after top surface cracking became visible. Only a few additional load coverages were necessary for the top slab surface to deteriorate from an uncracked to a complete failure condition. Relationships were established between load magnitude, prestressed pavement properties, and the number of coverages causing failure.
2. Strain and deflection data indicated that failures from the application of repeated moving loads were probably not caused by fatigue of the concrete in the top surface of the slab due to a repetition of radial tensile stresses. Rather, there appeared to be a progressive deterioration of the pavements caused by bottom surface cracks extending upward toward the top surface accompanied by increased deflections and a reduction in the concrete area needed to resist externally applied moments.
3. Static loads sufficient to cause top surface cracking were applied to two of the test slabs. Measured bottom surface cracking loads were accurately predicted by Westergaard's equation based on elastic theory. However, measured top surface cracking loads were greater than those predicted by existing methods of analysis for prestressed pavements.
4. Data from tests on slabs with varying magnitudes of prestress indicated that two-way prestress is required to avoid top surface cracking when relatively few moving loads greater than those causing bottom surface cracking are applied repeatedly at interior locations. Also, the minimum prestress required for prestressed concrete pavements to support repeated moving loads greater than those causing bottom surface cracking is approximately 30 psi.
5. Data from exploratory tests on slabs cast on foundations of different strengths indicated that an increase in the foundation strength resulted in an increase in the number of load coverages causing failure.
6. A fatigue factor, defined as moving wheel load divided by computed bottom surface cracking load, is suggested for evaluation of fatigue life of prestressed concrete

pavements. In practical design, this fatigue factor should be augmented by a suitable safety factor.

REFERENCES

1. Osawa, Y. Strength of Prestressed Concrete Pavements. Jour. Struct. Div., ASCE, Proc. Paper 3308, Vol. 88, No. ST5, p. 143-164, Oct. 1962; also, PCA Development Dept. Bulletin D57.
2. Christensen, A. P., and Janes, R. L. Load Tests on Thin Pretensioned Pavement Slabs. Highway Research Record 60, p. 77-94, 1964; also, PCA Development Dept. Bulletin D87.
3. Christensen, A. P. Load Tests on Post-Tensioned Pavement Slabs. Highway Research Record 60, p. 95-115, 1964; also, PCA Development Dept. Bulletin D88.
4. Hanson, N. W. Load Cells for Structural Testing. Jour. PCA R and D Labs., Vol. 1, No. 1, p. 40-44, 1959; also, PCA Development Dept. Bulletin D33.
5. Carlton, P. F., and Behrmann, R. M. Repetitive Loading Model Tests of Prestressed Rigid Pavement on a Low-Strength Subgrade. Corps of Engineers, Ohio River Div. Labs., Tech. Rept. No. 4-28, 1964.
6. Nowlen, W. J. Techniques and Equipment for Field Testing of Pavements. Jour. PCA R and D Labs., Vol. 6, No. 3, p. 43-52, Sept. 1964; also, PCA Development Dept. Bulletin D83.
7. Westergaard, H. M. New Formulas for Stresses in Concrete Pavements of Airfields. ASCE Proc. Vol. 75, p. 687-701, 1947.
8. Carlton, P. F. Small-Scale Model Studies of Prestressed Rigid Pavements for Military Airfields. Part II, Single-Wheel Loadings and Pre-Tensioned and Post-Tensioned Slabs. Corps of Engineers, Ohio River Div. Labs., Tech. Rept. No. 4-25, 1962.

Bulletins Published by the Development Department Research and Development Laboratories of the Portland Cement Association

D100—"Index of Development Department Bulletins D1-D99. Annotated List with Author and Subject Index."

Published by Portland Cement Association, Research and Development Laboratories, Skokie, Illinois (1967).

D101—"Rotational Capacity of Hinging Regions in Reinforced Concrete Beams," by ALAN H. MATTOCK.

Reprinted from FLEXURAL MECHANICS OF REINFORCED CONCRETE, *Proceedings of the International Symposium, Miami, Fla. (November 1964)* pages 143-181, joint sponsorship. Copyrighted 1965 by American Society of Civil Engineers.

D102—"Tests of Partially Prestressed Concrete Girders," by DONALD D. MAGURA and EIVIND HOGNESTAD.

Reprinted from the *Journal of the Structural Division, Proceedings of the American Society of Civil Engineers, Proc. Paper 4685,* **92,** *ST 1,* 327-350 (February 1966).

D103—"Influence of Size and Shape of Member on the Shrinkage and Creep of Concrete," by TORBEN C. HANSEN and ALAN H. MATTOCK.

Reprinted from *Journal of the American Concrete Institute* (February 1966); *Proceedings* **63,** 267-290 (1966).

D104—"Cast-in-Place Concrete Residences With Insulated Walls," by HARRY L. SCOGGIN.

Reprinted from *Journal of the PCA Research and Development Laboratories,* **8,** No. 2, 21-29 (May 1966).

D105—"Tensile Testing of Concrete Block and Wall Elements," by RICHARD O. HEDSTROM.

Reprinted from *Journal of the PCA Research and Development Laboratories,* **8,** No. 2, 42-52 (May 1966).

D106—"High Strength Bars as Concrete Reinforcement, Part 8. Similitude in Flexural Cracking of T-Beam Flanges," by PAUL H. KAAR.

Reprinted from *Journal of the PCA Research and Development Laboratories,* **8,** No. 2, 2-12 (May 1966).

D107—"Seismic Resistance of Reinforced Concrete—A Laboratory Test Rig," by NORMAN W. HANSON and HAROLD W. CONNER.

Reprinted from *Journal of the PCA Research and Development Laboratories,* **8,** No. 3, 2-9 (September 1966).

D108—"Rotational Capacity of Reinforced Concrete Beams," by W. GENE CORLEY.

Reprinted from *Journal of the Structural Division, Proceedings of the American Society of Civil Engineers, Proc. Paper 4939,* **92,** ST5, 121-146 (October 1966).

D109—"Laboratory Studies of the Skid Resistance of Concrete," by G. G. BALMER and B. E. COLLEY.

Reprinted from *ASTM Journal of Materials* **1,** No. 3, 536-559 (September 1966).

D110—"Connections in Precast Concrete Structures—Column Base Plates," by R. W. LAFRAUGH and D. D. MAGURA.

Reprinted from *Journal of the Prestressed Concrete Institute,* **11,** No. 6, 18-39 (December 1966).

D111—"Laboratory Study of Shotcrete," by ALBERT LITVIN and JOSEPH J. SHIDELER.

Reprinted from *Symposium on Shotcreting,* American Concrete Institute, Paper No. 13 in **Publication SP-14,** 165-184 (1966).

D112—"Tests on Soil-Cement and Cement-Modified Bases in Minnesota," by TORBJORN J. LARSEN.

Reprinted from *Journal of the PCA Research and Development Laboratories,* **9,** No. 1, 25-47 (January 1967).

D113—"Structural Model Testing—Reinforced and Prestressed Mortar Beams." by DONALD D. MAGURA.

Reprinted from *Journal of the PCA Research and Development Laboratories*, 9, No. 1, 2-24 (January 1967).

D114—"General Relation of Heat Flow Factors to the Unit Weight of Concrete," by HAROLD W. BREWER.

Reprinted from *Journal of the PCA Research and Development Laboratories*, 9, No. 1, 48-60 (January 1967).

D115—"Sand Replacement in Structural Lightweight Concrete—Sintering Grate Aggregates," by DONALD W. PFEIFER and J. A. HANSON.

Reprinted from *Journal of the American Concrete Institute* (March, 1967); *Proceedings* 64, 121-127 (1967).

D116—"Fatigue Tests of Reinforcing Bars—Tack Welding of Stirrups," by KENNETH T. BURTON and EIVIND HOGNESTAD.

Reprinted from *Journal of the American Concrete Institute* (May, 1967); *Proceedings* 64, 244-252 (1967).

D117—"Connections in Precast Concrete Structures—Effects of Restrained Creep and Shrinkage," by K. T. BURTON, W. G. CORLEY, and E. HOGNESTAD.

Reprinted from *Journal of the Prestressed Concrete Institute*, 12, No. 2, 18-37 (April, 1967).

D118—"Cast-in-Place Concrete Residences with Insulated Walls—Influence of Shear Connectors on Flexural Resistance," by HARRY L. SCOGGIN and DONALD W. PFEIFER.

Reprinted from *Journal of the PCA Research and Development Laboratories*, 9, No. 2, 2-7 (May 1967).

D119—"Fatigue of Soil-Cement," by T. J. LARSEN and P. J. NUSSBAUM.

Reprinted from *Journal of the PCA Research and Development Laboratories*, 9, No 2, 37-59 (May 1967).

D120—"Sand Replacement in Structural Lightweight Concrete—Splitting Tensile Strength," by DONALD W. PFEIFER.

Reprinted from *Journal of the American Concrete Institute* (July 1967); *Proceedings* 64, 384-392 (1967).

D121—"Seismic Resistance of Reinforced Concrete Beam-Column Joints," by NORMAN W. HANSON and HAROLD W. CONNER.

Reprinted from *Journal of the Structural Division, Proceedings of the American Society of Civil Engineers, Proc. Paper 5537*, 93, ST5, 533-560 (October 1967).

D122—"Precast Rigid Frame Buildings—Test of Scarf Connections," by PAUL H. KAAR and HAROLD W. CONNER.

Reprinted from *Journal of the PCA Research and Development Laboratories*, 9, No. 3, 34-42 (September 1967).

D123—"Precast Rigid Frame Buildings—Component Tests," by HAROLD W. CONNER and PAUL H. KAAR.

Reprinted from *Journal of the PCA Research and Development Laboratories*, 9, No. 3, 43-55 (September 1967).

D124—"Aggregate Interlock at Joints in Concrete Pavements," by B. E. COLLEY and H. A. HUMPHREY.

Reprinted from Highway Research RECORD, Number 189, 1-18 (1967).

D125—"Cement Treated Subbases for Concrete Pavements," by L. D. CHILDS.

Reprinted from Highway Research RECORD, Number 189, 19-43 (1967).

D126—"Sand Replacement in Structural Lightweight Concrete—Freezing and Thawing Tests," by DONALD W. PFEIFER.

Reprinted from *Journal of the American Concrete Institute* (November 1967); *Proceedings* 64, 735-744 (1967).

D127—"Ultimate Torque of Reinforced Rectangular Beams," by THOMAS T. C. HSU.

Reprinted from *Journal of the Structural Division, Proceedings of the American Society of Civil Engineers, Proc. Paper 5814*, 94, ST2, 485-510 (February 1968).

D128—"Sand Replacement in Structural Lightweight Concrete—Creep and Shrinkage Studies," by DONALD W. PFEIFER.

Reprinted from *Journal of the American Concrete Institute* (February 1968); *Proceedings*, 65, 131-140 (1968).

D129—"Shear and Moment Transfer Between Concrete Slabs and Columns," by NORMAN W. HANSON and JOHN M. HANSON.

Reprinted from *Journal of the PCA Research and Development Laboratories*, 10, No. 1, 2-16 (January 1968)

D130—"Trends in Consumer Demands for New Grades of Reinforcing Steel," by EIVIND HOGNESTAD.

Reprinted from *Proceedings*, Fall Business Meeting, Concrete Reinforcing Steel Institute, pages 22-32 (1967).

D131—"Influence of Mortar and Block Properties on Shrinkage Cracking of Masonry Walls," by RICHARD O. HEDSTROM, ALBERT LITVIN, and J. A. HANSON.

Reprinted from *Journal of the PCA Research and Development Laboratories*, 10, No. 1, 34-51 (January 1968).

D132—"Toward a Generalized Treatment of Delayed Elasticity in Concrete," by DOUGLAS MCHENRY.

Reprinted from PUBLICATIONS, International Association for Bridge and Structural Engineering (Zurich), Vol 26, pages 269-283 (1966).

D133—"Torsion of Structural Concrete—A Summary of Pure Torsion," by THOMAS T. C. HSU.

Reprinted from TORSION OF STRUCTURAL CONCRETE, American Concrete Institute, Paper SP 18-6 in **Publication SP-18**, 165-178 (1968).

D134—"Torsion of Structural Concrete—Plain Concrete Rectangular Sections," by THOMAS T. C. HSU.

Reprinted from TORSION OF STRUCTURAL CONCRETE, American Concrete Institute, SP 18-8 in **Publication SP-18**, 203-238 (1968).

D135—"Torsion of Structural Concrete—Behavior of Reinforced Concrete Rectangular Members," by THOMAS T. C. HSU.

Reprinted from TORSION OF STRUCTURAL CONCRETE, American Concrete Institute, Paper SP 18-10 in **Publication SP-18, 261-306 (1968).**

D136—"Precast Rigid Frame Buildings—Summary of a Laboratory Investigation," by PAUL H. KAAR and HAROLD W. CONNER.

Reprinted from *Journal of the PCA Research and Development Laboratories*, 10, No. 2, 25-34 (May 1968).

D137—"Clear Coatings for Exposed Architectural Concrete," by ALBERT LITVIN.

Reprinted from *Journal of the PCA Research and Development Laboratories*, 10, No. 2, 49-57 (May 1968).

D138—"Torsion of Structural Concrete—Interaction Surface for Combined Torsion, Shear, and Bending in Beams Without Stirrups," by THOMAS T. C. HSU.

Reprinted from *Journal of the American Concrete Institute* (January 1968); *Proceedings*, 65, 51-60 (1968).

D139—"Influence of Aggregate Properties on Effectiveness of Interlock Joints in Concrete Pavements," by W. J. NOWLEN.

Reprinted from *Journal of the PCA Research and Development Laboratories*, 10, No. 2, 2-8 (May 1968).

D140—"Torsion of Structural Concrete—Uniformly Prestressed Rectangular Members Without Web Reinforcement," by THOMAS T. C. HSU.

Reprinted from *Journal of the Prestressed Concrete Institute*, 13, No. 2, 34-44 (April 1968).

D141—"Effects of Curing and Drying Environments on Splitting Tensile Strength of Concrete," by J. A. HANSON.

Reprinted from *American Concrete Institute* (July 1968); *Proceedings*, 65, 535-543 (1968).

D142—"Research on Thickness Design for Soil-Cement Pavements," by T. J. LARSEN, P. J. NUSSBAUM, and B. E. COLLEY.

Published by Portland Cement Association, Research and Development Laboratories, Skokie, Illinois (1969).

D143—"Fatigue Tests of Prestressed Concrete Pavements," by A. P. CHRISTENSEN and B. E. COLLEY.

Reprinted from *Highway Research Record*, Number 239, 175-196 (1968).

Printed in U.S.A.

"Fatigue Tests of Prestressed Concrete Pavements."

KEYWORDS: Deflection; design; fatigue (materials); models; moving loads; prestressed concrete pavements; stresses; subgrade; theories.

SYNOPSIS: The fatigue characteristics of prestressed concrete pavements were studied by a program of repetitive moving load tests of 16 reduced scale prestressed concrete slabs. Relationships were established between load magnitude, prestressed pavement properties, and the number of load coverages causing failure. Data from tests on slabs with varying magnitudes of prestress indicate that a minimum two-way prestress of approximately 30 psi is required to support repeated, moving, interior loads greater than those causing bottom surface cracking. Data from tests on slabs cast on foundations of different strengths indicated that an increase in the foundation strength resulted in an increase in the number of load coverages causing failure.

REFERENCE: Christensen, A. P., and Colley, B. E., "Fatigue Tests of Prestressed Concrete Pavements, Highway Research RECORD Number 239, 175-196 (1968); *PCA Development Department Bulletin D143.*

"Fatigue Tests of Prestressed Concrete Pavements."

KEYWORDS: Deflection; design; fatigue (materials); models; moving loads; prestressed concrete pavements; stresses; subgrade; theories.

SYNOPSIS: The fatigue characteristics of prestressed concrete pavements were studied by a program of repetitive moving load tests of 16 reduced scale prestressed concrete slabs. Relationships were established between load magnitude, prestressed pavement properties, and the number of load coverages causing failure. Data from tests on slabs with varying magnitudes of prestress indicate that a minimum two-way prestress of approximately 30 psi is required to support repeated, moving, interior loads greater than those causing bottom surface cracking. Data from tests on slabs cast on foundations of different strengths indicated that an increase in the foundation strength resulted in an increase in the number of load coverages causing failure.

REFERENCE: Christensen, A. P., and Colley, B. E., "Fatigue Tests of Prestressed Concrete Pavements, Highway Research RECORD Number 239, 175-196 (1968); *PCA Development Department Bulletin D143.*

"Fatigue Tests of Prestressed Concrete Pavements."

KEYWORDS: Deflection; design; fatigue (materials); models; moving loads; prestressed concrete pavements; stresses; subgrade; theories.

SYNOPSIS: The fatigue characteristics of prestressed concrete pavements were studied by a program of repetitive moving load tests of 16 reduced scale prestressed concrete slabs. Relationships were established between load magnitude, prestressed pavement properties, and the number of load coverages causing failure. Data from tests on slabs with varying magnitudes of prestress indicate that a minimum two-way prestress of approximately 30 psi is required to support repeated, moving, interior loads greater than those causing bottom surface cracking. Data from tests on slabs cast on foundations of different strengths indicated that an increase in the foundation strength resulted in an increase in the number of load coverages causing failure.

REFERENCE: Christensen, A. P., and Colley, B. E., "Fatigue Tests of Prestressed Concrete Pavements, Highway Research RECORD Number 239, 175-196 (1968); *PCA Development Department Bulletin D143.*